Noiser: Bounded Input Perturbations for Attributing Large Language Models

Mohammad Reza Ghasemi Madani[1]* **Aryo Pradipta Gema**[2] **Gabriele Sarti**[3]
Yu Zhao[2] **Pasquale Minervini**[2,4] **Andrea Passerini**[1]
[1]University of Trento [2]University of Edinburgh [3]CLCG, University of Groningen
[4] Miniml.AI

Abstract

Feature attribution (FA) methods are common post-hoc approaches that explain how Large Language Models (LLMs) make predictions. Accordingly, generating faithful attributions that reflect the actual inner behavior of the model is crucial. In this paper, we introduce **NOISER**, a perturbation-based FA method that imposes bounded noise on each input embedding and measures the robustness of the model against partially noised input to obtain the input attributions. Additionally, we propose an *answerability* metric that employs an instructed judge model to assess the extent to which highly scored tokens suffice to recover the predicted output. Through a comprehensive evaluation across six LLMs and three tasks, we demonstrate that Noiser consistently outperforms existing gradient-based, attention-based, and perturbation-based FA methods in terms of both faithfulness and answerability, making it a robust and effective approach for explaining language model predictions.[1]

1 Introduction

Transformer-based language models (Vaswani et al., 2023) are fundamental to the latest advancements in natural language processing (Team et al., 2024; Touvron et al., 2023; Bai et al., 2023; DeepSeek-AI, 2025; OpenAI et al., 2024). However, they are often perceived as opaque (Rudin, 2019; Doshi-Velez & Kim, 2017; Lipton, 2018), sparking significant interest in the development of algorithms that can automatically explain the behavior of these models (Denil et al., 2015a; Sundararajan et al., 2017a; Camburu et al., 2018; Rajani et al., 2019; Luo et al., 2022).

Feature attribution (FA) techniques are popular post-hoc methods that generate token-level importance scores to highlight the contribution of each token to a prediction (Denil et al., 2015b; Jain et al., 2020; Kersten et al., 2021). The top-p% important tokens are typically considered as the prediction rationale (Zaidan et al., 2007; Sundararajan et al., 2017b; DeYoung et al., 2020). The quality of a rationale is often evaluated using *faithfulness* metrics, which measure to what extent the rationales accurately reflect the downstream task on model predictions.

Perturbation-based FA methods aim to explore neural networks by modifying the input of a model and observing the changes in the output to indicate which parts of the input are particularly important for inference. These methods are widely adopted in computer vision, leveraging the continuous nature of image inputs, where localized noise or masking preserves semantic coherence and avoids distribution shifts (Ivanovs et al., 2021). In contrast, NLP models face inherent challenges due to the discrete structure of the text, where even minor perturbations—whether token substitutions or embedding modifications—can push inputs out-of-distribution (OOD), destabilizing predictions and confounding attribution analysis (Liu et al., 2019).

*Correspondence to: rezamadani.ai@gmail.com.

[1] Our code: https://github.com/qasemii/Noiser

This divergence underscores the need for bounded perturbations in NLP, ensuring perturbed inputs remain in-distribution. Our work bridges this gap by exploring noise thresholds that alter token embeddings while preserving the original prediction to limit perturbation-induced OOD issues. Particularly, we introduce a perturbation-based FA by exploring a model's robustness against *noisy inputs*—examples created by introducing small alterations to the input embeddings without changing the model's original prediction—enabling reliable explanations grounded in the model's trained operational domain while quantifying feature importance through robustness to controlled perturbations. Our work makes the following contributions:

- We empirically show that NOISER is consistently more faithful than nine popular FAs by conducting comprehensive experiments, covering three tasks and six LMs of varying sizes from three different model families;
- We propose a new plausibility metric, *answerability*, which measures the extent to which the top-p% attributed input tokens sufficiently support the target output. By leveraging language models, this metric assesses whether a minimal subset of input tokens is adequate for generating the expected prediction, providing a simulatable alternative to human plausibility judgments.

2 Background

2.1 Generative Language Modeling

In generative language modeling, the input consists of a sequence of tokens, denoted as $\mathrm{X} = [x_0, \ldots, x_{T-1}]$. The objective is to develop a model, $\mathcal{F}\theta$, that estimates the probability distribution P over the token sequence X. In this context, $\mathcal{F}\theta$ represents a specific pre-trained generative language model characterized by parameters θ.

$$P(x_0, \ldots, x_{T-1}) = \mathcal{F}_\theta(x_0) \prod_{t=1}^{T-1} \mathcal{F}_\theta(x_t \mid x_0, \ldots, x_{t-1})$$

2.2 Input Importance for Generative LMs

Given a model $\mathcal{F}_\theta$, our objective is to determine the importance distribution of the input tokens for each predicted token x_T, based on the preceding sequence $\mathrm{X} = [x_0, \ldots, x_{T-1}]$. A feature attribution method, denoted as e_T, applied at position T, yields an importance distribution $\mathrm{S}_T = [s_0, \ldots, s_{T-1}]$ corresponding to the target token x_T, where a higher value of s_i indicates greater importance of the input token x_i in predicting x_T.

$$e_T(\mathcal{F}_\theta, \mathrm{X}, x_T) \rightarrow \mathrm{S}_T$$

2.3 Bounded Perturbations

Bounded perturbations refer to small, structured uncertainties in mathematical systems where a specified constraint limits the perturbation magnitude. These are critical for analyzing system robustness against disturbances while ensuring predictable behavior.

Perturbation is a minor alteration to a system, such as δ added to a nominal matrix A, resulting in $A + \delta$. This captures uncertainties or disturbances. If the perturbation magnitude is bounded as $\|\delta\| \leq \epsilon$, where $\epsilon > 0$, it is called a bounded perturbation. Consider the nominal system $\dot{x} = Ax$. Under a perturbation δ, the system becomes:

$$\dot{x} = (A + \delta)x.$$

3 Our Method

Let $\mathbf{n} \in \mathbb{R}^{d_{\text{model}}}$ denote a noise vector where each component $n_i \sim \mathcal{N}(0, 1)$. We form noisy examples from original inputs by imposing small perturbations to the input embeddings, such that the noisy input results in the model outputting an incorrect answer. For this purpose, we first pass a prompt $\mathrm{X} = [x_0, \ldots, x_{T-1}]$ into $\mathcal{F}_\theta$ to collect the probability distribution, P, over the model's vocabulary with x_T being the most likely output (*i.e.*, $\mathcal{F}_\theta(\mathrm{X}) = x_T$).

In the next step, we utilize a *binary search* algorithm to find the **maximum** scaling factor k such that if we perturb the embedding of a targeted token with $\mathbf{n}_{\text{scaled}} = k \cdot \mathbf{n}$ the model wouldn't change its initial prediction x_T. Specifically, we set $x_i := x_i + \mathbf{n}_{\text{scaled}}$ and let $\mathcal{F}_\theta$ to continue, giving us a set of corrupted probabilities $P^*_{x_i}$. Because $\mathcal{F}_\theta$ partially loses information about the corrupted token, the probability of x_T from the first step would likely be lower in $P^*_{x_i}$.

We repeat the process for each token until we obtain $\mathrm{K} = [k_0, \ldots, k_{T-1}]$ where each k_i is the maximum scaling factor such that if we corrupt the embeddings of x_i using $\mathbf{n}_{\text{scaled}} = k_i \cdot \mathbf{n}$, the model wouldn't change its original output. The mathematical representation of K is illustrated below:

$$K = \{k_i \mid \forall k > k_i \Rightarrow \mathcal{F}_\theta(\mathrm{X}^i_{\text{perturbed}|k}) \neq x_T, \mathcal{F}_\theta(\mathrm{X}^i_{\text{perturbed}|k_i}) = x_T\}, \quad i \in \{0, \ldots, t-1\}$$

where $\mathrm{X}^i_{\text{perturbed}|k} = [x_0 \ldots (x_i + \mathbf{n}_{\text{scaled}}) \ldots x_{t-1}]$ is the input sequence in which x_i is altered with $\mathbf{n}_{\text{scaled}} = k \cdot \mathbf{n}_{\text{bounded}}$. The equation above indicates that each scale factor k_i is such that for all values k greater than k_i if we perturb x_i using $\mathbf{n}_{\text{sclaed}} = k \cdot \mathbf{n}_{\text{bounded}}$ to create a noisy input $\mathrm{X}^i_{\text{perturbed}|k}$, $\mathcal{F}_\theta$ would return a different output from the original one (x_T).

In the final step, we find the $k_{\min} = \min(K)$ to generate the final noise samples $\mathbf{n}_{\text{scaled}} = k_{\min} \cdot \mathbf{n}$ to add to each token embedding and obtain the token scores using the following:

$$S = \{s_i \mid s_i = p(\mathrm{X}) - p(\mathrm{X}^i_{\text{perturbed}|k_{\min}})\}, \quad i \in \{0, \ldots, t-1\}$$

Using $k_{\min}$, we ensure to perturb the input enough to reach a flipping point in prediction to get the minimal set of features needed to achieve this outcome. The intuition is that tokens with higher importance are more sensitive to noise injection, resulting in a larger reduction in the model's output likelihood.

To show the effectiveness of selecting $k_{\min}$, we propose different boundings and measure their faithfulness. We analyse **i)** using maximum noise across tokens ($k_{\max}$); **ii)** individual token maximum noise where k is different for each input token and is the maximum the model can tolerate ($k_{\max}$ per token); **iii)** norm-bounded setting where the noise vector $\mathbf{n}$ is divided by the expected value of the noise vector L_p norm, $\mathbb{E}\left[\|\mathbf{n}\|_p\right]$; and **iv)** random k where k is randomly selected from the uniform distribution. The details of each configuration are provided in Section 5.

4 Experiment

4.1 Model & Data

In our study, we employ variants of Qwen (Bai et al., 2023), Gemma (Team et al., 2024), and Llama (Touvron et al., 2023) models. We choose our models to span from hundreds of millions to a few billion parameters as we want to explore how the model size affects the faithfulness of each FA. All models used are publicly available. [2]

We use Known dataset[3] provided by Meng et al. (2023) and Long-Range Agreement (LongRA; Vafa et al., 2021) to conduct our analysis. Besides, for long generation we utilize WikiBio (Lebret et al., 2016). The following is an instance from the Known dataset.

[2] We use checkpoints from the Huggingface library for each model.

[3] Dataset can be found at: `https://rome.baulab.info/data/dsets/known_1000.json`

> *LeBron James professionally plays the sport of* [***basketball***]

The LongRA dataset consists of word pairs that exhibit either a semantic or syntactic relationship. Additionally, Vafa et al. (2021) incorporate a distractor sentence, which provides no relevant information about the word pair, to evaluate long-range agreement. An example from the LongRA dataset is shown below, with the distractor included in parentheses.

> *When my flight landed in* ***Japan****, I converted my currency and slowly fell asleep. (I had a terrifying dream about my grandmother, but that's a story for another time). I was staying in the* ***capital****,* [***Tokyo***]

WikiBio is a dataset consisting of Wikipedia biographies. We use the first two sentences as a prompt, similar to Manakul et al. (2023). The model is then expected to continue generating the biography. This task is inherently more open-ended compared to the previous two.

> *Super Mario Land is a 1989 side-scrolling platform video game*

The computation of each task's faithfulness is provided in Section 4.5.

4.2 Baselines

Following previous works, we compare our rationalization method to a variety of gradient- and attention-based baselines (Vafa et al., 2021). **Input×Gradient** (Denil et al., 2015b) uses embedding gradients multiplied by the embeddings; **Integrated Gradients** (Sundararajan et al., 2017b) integrate overall gradients using a linear interpolation between a baseline input (all zero embeddings) and the original input. **Gradient SHAP** (Lundberg & Lee, 2017) compute the gradient w.r.t. randomly selected points between the inputs and a baseline distribution; **DeepLIFT** (Shrikumar et al., 2019) compares the activation of each neuron to its 'reference activation' and assigns contribution scores according to the difference. **Sequential Integrated Gradients** (Enguehard, 2023) extends Integrated Gradients by breaking down the input perturbation into sequential steps, computing gradients at each step, and aggregating them to provide more stable and interpretable attributions, **Last Attention** (Jain et al., 2020) uses the last-layer attention weights averaged across heads; **Attention Rollout** (Abnar & Zuidema, 2020) recursively computing the token attention in each layer, e.g., computing the attention from all positions in layer l_i to all positions in layer l_j, where $j < i$; **LIME** (Ribeiro et al., 2016) trains a linear surrogate model using data points randomly sampled locally around the prediction. **Occlusion** (Zeiler & Fergus, 2014) involves systematically occluding different portions of the input and observing the impact on the output confidence.

4.3 Faithfulness Metrics

To assess whether a rationale extracted with a given FA is faithful, *i.e.,* actually reflects the true model reasoning (Jacovi & Goldberg, 2021), various faithfulness metrics have been proposed (Arras et al., 2017; Serrano & Smith, 2019; Jain et al., 2020; DeYoung et al., 2020). Sufficiency and comprehensiveness (DeYoung et al., 2020) are two widely used metrics that effectively capture rationale faithfulness (Chrysostomou & Aletras, 2021; Chan et al., 2022b). Both metrics use a hard erasure criterion for perturbing the input by entirely removing (*i.e.,* comprehensiveness) or retaining (*i.e.,* sufficiency) the rationale to observe changes in predictive likelihood. This hard criterion ignores the importance of each individual token, treating them all equally for computing sufficiency and comprehensiveness.

We evaluate rationales using soft sufficiency (Soft-NS) and comprehensiveness (Soft-NC) proposed by Zhao & Aletras (2023) to measure the faithfulness of the full importance distribution. Using these metrics, instead of entirely removing or retaining tokens from the input, we randomly mask parts of the token vector representations proportionately to their FA importance. The summation of Soft-NC and Soft-NS is considered as the final faithfulness score. For the detailed implementation of these metrics, please refer to Appendix A.

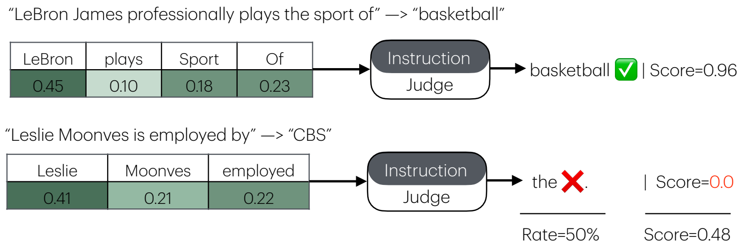

Figure 1: Answerability metrics evaluation. To get the answerability metrics, the judge model is instructed to predict the completion token given a limited set of tokens from the original prompt.

4.4 Answerability Metrics

The utilization of LLMs has emerged as a prominent trend across numerous research domains (Peng et al., 2023; Zhou et al., 2023a; Taori et al., 2023). With any given instructions, LLMs are expected to generate responses that align with these instructions (Chen et al., 2024; Li et al., 2024; Xu et al., 2023; Longpre et al., 2023).

This capability, known as the "instruction following" ability, serves as a key metric for assessing the effectiveness of LLMs (Chen et al., 2024; Zhao et al., 2024; Taori et al., 2023; Zheng et al., 2023). To facilitate a more thorough assessment, several benchmarks have been introduced with a focus on instruction following (Zhou et al., 2023b; Qin et al., 2024).

We exploit this progress in our answerability metric by framing attribution evaluation as an instruction-based completion task. To see whether the attributions illustrate any meaningful association with a predicted output, we extend our evaluation of FAs through prompt engineering. For this purpose, we aggregate the attribution scores of each word's sub-tokens to derive word-level scores. Then we select the top-p% most important words w.r.t. their scores and feed these words as input to a judge model along with a task prompt. The task prompt asks the judge model to predict the completion token using this limited set of words. Feldhus et al. (2023) offer a complementary perspective—while they leverage LLMs for generating interpretability-enhancing verbalizations, our approach instead uses an LLM to directly quantify whether the selected tokens are sufficient for the prediction task.

We evaluate attributions by computing the number of samples for which the judge model generates the correct output, which we define as the FAs ***answerability rate***. Additionally, for these correctly predicted samples, we aggregate the word-level attribution scores to obtain the so-called ***answerability score***. For both metrics, higher values indicate better performance. In our evaluation, a higher answerability rate means that a larger proportion of samples allow the LM judge to correctly predict the output using only the minimal set of tokens. Likewise, a higher answerability score—reflecting a greater aggregated attribution mass within that token set—indicates that the attribution method is more effective at isolating the minimal semantic requirements for prediction.

This evaluation pipeline specifically applies to datasets such as KNOWN where the gold label is a meaningful word that must be inferred from the input sequence. Figure 1 shows an answerability evaluation example. The prompt used for this evaluation is shown in Appendix E.

4.5 Implementation Details

None of our experiments involved training or fine-tuning any language models. All FAs are built upon Inseq library (Sarti et al., 2023; 2024) except Last Attention and Attention Rollout, which we used the codebase from Zhao & Shan (2024). For NOISER, we generate 10 different noise vectors during the corrupted run for more consistent results. Binary search is done in 10 steps, yielding the accuracy of ≈ 0.001 for the scaling factor (k). For KNONW and

KNOWN

Method	Qwen2-0.5B	Llama3.2-1B	Qwen2-1.5B	gemma-2-2B	gemma-2-9B	Llama3-8B	Average
Last Attn	-0.0857	-0.0601	0.0607	0.1407	-0.2788	-0.0095	-0.0388
Rollout	-0.1161	-0.0471	0.1211	0.4624	-0.3607	-0.2625	-0.0338
SHAP	0.4946	0.3746	0.5390	0.3726	0.9203	0.1925	0.4823
IxG	0.2117	0.7059	0.4612	0.5233	1.0276	0.5891	0.5865
IG	0.2176	0.5428	0.5163	0.2015	1.0355	0.3759	0.4816
DeepLIFT	0.3030	0.5473	0.5323	0.3557	0.8638	0.5174	0.5199
SIG	0.0361	0.3534	0.3003	-0.1879	0.7877	0.2755	0.2609
LIME	0.2439	0.5103	0.3826	0.3567	0.4832	0.6555	0.4392
Occlusion	0.1627	0.5373	0.2477	0.5341	0.5221	0.7831	0.4645
NOISER	**2.1854**	**1.3989**	**1.4400**	**1.4433**	**2.1767**	**2.2175**	**1.8103**

LONGRA

Method	Qwen2-0.5B	Llama3.2-1B	Qwen2-1.5B	gemma-2-2B	gemma-2-9B	Llama3-8B	Average
Last Attn	1.9148	0.3255	-0.0110	-0.2382	-0.2382	1.0762	0.4715
Rollout	1.8517	0.2451	0.0802	-0.2643	-0.2643	1.2283	0.4794
SHAP	3.7970	1.2837	1.6276	1.9746	2.2769	0.7696	1.9549
IxG	3.8972	1.7299	1.5370	2.5803	2.5803	2.0796	2.4007
IG	4.3388	1.3066	1.5498	1.3023	1.3023	3.7190	2.2531
DeepLIFT	4.4991	1.7889	1.5512	2.7428	2.7428	2.1258	2.5751
SIG	3.8645	0.9272	1.1047	0.5412	0.5412	1.1618	1.3568
LIME	1.0765	0.2212	-0.4147	-0.1636	-0.1636	2.2995	0.4759
Occlusion	3.9424	1.9887	1.0145	3.4418	3.4418	4.2240	3.0089
NOISER	**6.8055**	**4.8072**	**3.1779**	**4.2727**	**6.1681**	**5.1627**	**5.0657**

WIKIBIO

Method	Qwen2-0.5B	Llama3.2-1B	Qwen2-1.5B	gemma-2-2B	gemma-2-9B	Llama3-8B	Average
Last Attn	1.0605	0.6304	-0.7054	-0.2579	0.2815	0.5500	0.2598
Rollout	-0.6404	0.5591	-0.7066	0.5085	0.3498	0.8785	0.1582
SHAP	1.4702	1.1672	1.1213	0.7966	3.1494	1.4063	1.5185
IxG	3.4273	1.8365	1.3942	1.5816	2.6047	1.3747	2.0365
IG	2.4216	1.5797	0.6975	1.1909	4.1117	0.6876	1.7815
DeepLIFT	3.2207	1.6265	1.4590	1.4607	2.3006	1.2739	1.8903
SIG	3.7656	1.4300	2.0816	1.4256	5.2280	1.3620	2.5488
LIME	3.0009	0.5656	1.1714	0.7180	2.9527	0.8349	1.5406
Occlusion	5.1051	2.0019	3.8916	2.7232	4.9300	3.3885	3.6734
NOISER	**8.7624**	**3.7385**	**4.9864**	**4.2527**	**7.1509**	**4.6089**	**5.5833**

Table 1: Faithfulness scores across tasks.

LONGRA datasets, where the models must provide a single output, we filter down samples to the ones that the model can correctly generate the gold output. See Appendix C for the details. For WIKIBIO, we generate 10 tokens for input completion. To obtain the faithfulness score in this task, we compute the faithfulness of each next token w.r.t. all the previous tokens and consider the averaged score as the final faithfulness. The judge model used to get the answerability metrics is `Llama-3.3-70B-Instruct-Turbo`. We chose the top-50% of the most important words from the input prompt to get the answerability score and rate.

5 Results

Table 1 presents the faithfulness scores across different tasks. Following Zhao & Shan (2024), each score is computed as the logarithm of the ratio between the method's score and the random baseline. Consequently, scores below zero indicate less faithful methods than the random baseline, *i.e.,* unfaithful. As shown in Table 1, faithfulness varies across different FA methods and generative models. Notably, NOISER consistently achieves higher faithfulness scores across all tasks and models, outperforming traditional FAs. This suggests that NOISER provides more reliable attributions, reinforcing its effectiveness in evaluating model faithfulness.

To demonstrate the effectiveness of selecting k_{min}, we compare its faithfulness performance against alternative bounding strategies across different models in Table 2. The results show

Scaling Factor (k)	**Qwen2-0.5B**	**Llama3.2-1B**	**Qwen2-1.5B**	**gemma-2-2B**	**gemma-2-9B**	**Llama3-8B**	**Average**
random k	1.1519	1.0993	0.7165	1.2287	1.6007	1.4522	1.2082
None ($k = 1$)	1.0922	1.0219	0.6445	1.1844	1.4726	1.1070	1.0871
$\mathbb{E}\left[\lVert\mathbf{n}\rVert_2\right]^{-1}$	1.4849	1.3031	1.2617	1.7236	2.7905	1.7470	1.7185
$\mathbb{E}\left[\lVert\mathbf{n}\rVert_\infty\right]^{-1}$	0.8989	0.9515	0.7164	1.1275	1.4300	1.4115	1.0893
k_{max} per token	1.2230	0.9938	0.5850	1.2897	1.8359	1.0984	1.1710
k_{max}	1.0962	1.0203	0.6515	1.1824	1.4753	1.1059	1.0886
k_{min}	**2.1854**	**1.3989**	**1.4400**	1.4433	2.1767	**2.2175**	**1.8103**

Table 2: Comparison of different boundings on the faithfulness score on KNOWN dataset.

Method	**Qwen2-0.5B**		**Llama3.2-1b**		**Qwen2-1.5B**		**gemma-2-2b**		**gemma-2-9b**		**Llama3-8b**		**Average**	
	Rate	**Score**	**Rate**	**Score**	**Rate**	**Score**	**Rate**	**Score**	**Rate**	**Score**	**Rate**	**Score**	**Rate**	**Score**
Last Attn	14%	0.0936	48%	0.2496	10%	0.0670	39%	0.2064	37%	0.1854	39%	0.2081	31%	0.1684
Rollout	8%	0.0527	13%	0.0649	8%	0.0557	9%	0.0457	22%	0.1033	27%	0.1364	16%	0.0812
SHAP	22%	0.1805	29%	0.1890	24%	0.1862	17%	0.1249	11%	0.0764	26%	0.1454	22%	0.1504
IxG	27%	0.2177	33%	0.2412	26%	0.1942	35%	0.2408	35%	0.2537	30%	0.2079	31%	0.2259
IG	20%	0.1638	28%	0.1827	18%	0.1426	16%	0.1197	12%	0.0875	27%	0.1360	20%	0.1387
DeepLIFT	21%	0.1753	34%	0.2279	26%	0.1991	32%	0.2225	30%	0.2107	31%	0.2019	29%	0.2062
SIG	21%	0.1583	21%	0.1271	20%	0.1520	9%	0.0617	26%	0.1978	12%	0.0627	18%	0.1266
LIME	37%	0.2986	25%	0.1692	41%	0.3308	45%	0.3003	50%	0.3291	36%	0.2423	39%	0.2784
Occlusion	53%	0.3689	**49%**	0.3223	**54%**	**0.4224**	**48%**	0.3152	**52%**	0.3323	**50%**	0.3726	**51%**	0.3556
NOISER	**55%**	**0.5063**	37%	**0.3665**	43%	0.4099	43%	**0.4102**	49%	**0.4497**	41%	**0.4858**	45%	**0.4381**

Table 3: Answerability metrics on KNOWN dataset w.r.t. judge model top-1 predition.

that k_{min} consistently yields the highest faithfulness scores, confirming its superiority in preserving model behavior under noise perturbation.

Since k_{min} is model-dependent, we introduce norm-bounding as a flexible alternative, where the noise vector $\mathbf{n}$ is scaled based on the model's embedding size (see Appendix D). We further compare our approach with k_{max}, which applies the maximum k across all input tokens ($\max(K)$), and a variant, k_{max} per token, which applies a per-token maximum scaling factor. The latter performs slightly better, as it results in a less aggressive perturbation than the global k_{max}, reducing the likelihood of extreme changes in model behavior.

Additionally, we analyze the effects of unbounded scaling ($k = 1$) and random k, where k is sampled from a uniform distribution for each input sample. The consistently lower faithfulness scores in these settings highlight the necessity of proper bounding strategies to maintain faithfulness.

Overall, k_{min} is the only configuration that guarantees the model does not change its prediction under noise, making it the most reliable choice. The detailed computation of expected norm values is provided in Appendix D.

In addition to faithfulness, we monitored the runtime efficiency of NOISER and compared it with other FA methods. As expected, attention-based methods were the fastest, followed by gradient-based methods. On the other hand, perturbation-based techniques are generally more computationally demanding. However, the runtime of NOISER can be further reduced by decreasing the number of binary search steps (e.g., from 10 to 5), which yields a noticeable speed-up with only a slight trade-off in faithfulness.

The *answerability* rate and score are reported in Table 3. While NOISER achieves the highest answerability score in most cases and on average, Occlusion attains the highest answerability rate. This indicates that when NOISER attributions are deemed answerable (rate), the importance scores assigned to the top-p% tokens are significantly high, which is desirable. In contrast, Occlusion produces a higher number of answerable attributions but with lower scores, implying that it does not assign as much weight to key tokens.

To provide a more flexible analysis of answerability metrics, we examine cases where the gold prediction appears within the top-5 predictions of the judge model. Under this evaluation, the gap between NOISER's answerability score and those of other baselines widens, while its answerability rate also improves and approaches that of Occlusion, which achieves the best rate.

To further contextualize the answerability metrics, we also analyzed the answerability rate when all tokens (top-100%) are provided to the judge model. This represents an upper bound on the judge model's performance, offering insight into how often the judge model itself can recover the gold prediction using the full input. In our case, using all tokens, the judge model achieves approximately 84% accuracy when considering only the top-1 prediction, and around 92% accuracy when allowing for the gold output to appear among the top-5 predictions. This highlights the intrinsic limitations of the judge model and provides a reference point when interpreting answerability rates obtained from top-p% subsets.

Another aspect regarding the FA methods' efficiency that we evaluate is their ability to identify the minimal set of tokens most relevant to the output. We visualize the importance scores assigned by each method to critical tokens in the LONGRA "country-capital" category. Additionally, we examine the distribution of importance scores across the distractor and main parts in Figure 2. As shown in Figure 2, NOISER assigns the highest importance to critical tokens while effectively disregarding the distractor section, demonstrating a stronger focus on the main part compared to the best-performing baselines.

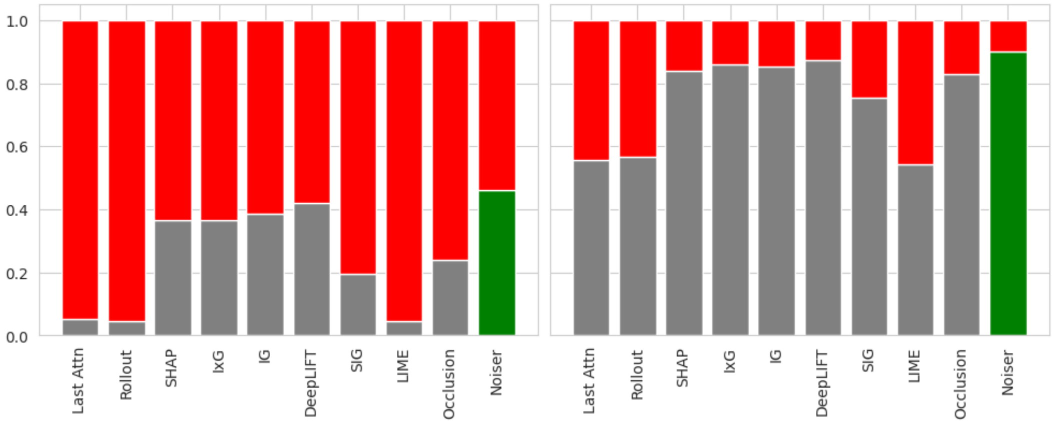

Figure 2: The aggregated score that each FAs put different parts of inputs from the "capital-world" subclass in LONGRA dataset. The red indicates the score assigned to the undesired part (e.g., distractor). The left image illustrates the aggregated score on "country"+"capital" token. The right image indicates the overall score on the main part against the distractor.

Finally, we analyzed the minimum proportion of top attributions required for each FA method to ensure that the judge model correctly predicts the original output. To determine this value, we first computed attributions for each sample using a given FA method. Then, starting with the full set of tokens, we iteratively removed the least important tokens one by one until the judge model produced an incorrect prediction. We repeated this process across all samples, averaging the proportion of retained tokens to obtain the final minimum top-p% required for accurate prediction. A lower value indicates a more effective FA method in identifying the most relevant attributions. In this regard, Occlusion requires the least number of tokens overall, which aligns with the results in Table 3, while Lime and NOISER take the second and third best place with minimal difference.

6 Related Works

Post-hoc explanation methods, such as FA techniques, are applied retrospectively by seeking to extract explanations after the model makes a prediction. Most FAs have been proposed in the context of classification tasks, where a sequence input $X = [x_0, \ldots, x_{t-1}]$ is associated with a true label y and a predicted label $\hat{y}$. The underlying goal is to identify which parts of the input contribute more toward the prediction $\hat{y}$ (Atanasova et al., 2020; Wallace et al., 2020; Madsen et al., 2022; Chrysostomou & Aletras, 2022; Lei et al., 2016; Chan et al., 2022a; Ghasemi Madani & Minervini, 2023). Most FAs generally fall into gradient, attention, and perturbation-based categories.

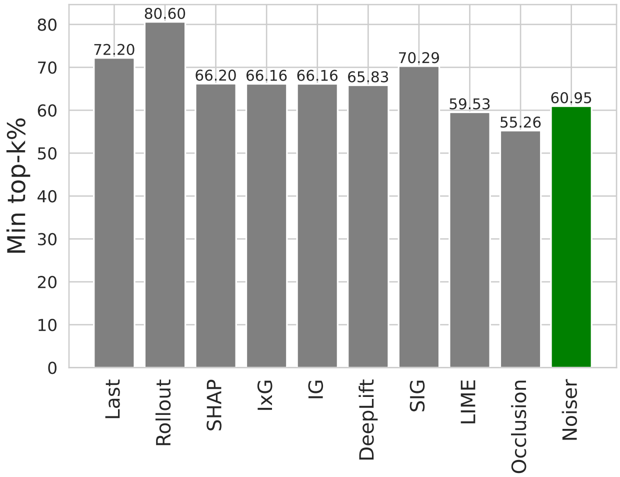

Figure 3: Minimum top-p% attribution required for the judge model to retain the correct prediction across different feature attribution methods. Lower values indicate higher attribution accuracy, as fewer tokens are needed to maintain the original output.

Dataset	Input	Output
Known	LeBron James professionally plays the sport of	basketball
LongRA	When my flight landed in Japan , I converted my currency and slowly fell asleep . (I had a terrifying dream about my grandmother , but that ’ s a story for another time) . I was staying in the capital ,	Tokyo
WikiBio	Super Mario Land is a 1989 side-scrolling platform video game developed and published by	Nintendo

Table 4: Example of NOISER attributions on different inputs.

Gradient-based methods derive the importance for each token by computing gradients w.r.t. the input (Denil et al., 2015b). The resulting gradient captures intuitively the *sensitivity* of the model to each element in the input when predicting token w. While attribution scores are computed for every dimension of input token embeddings, they are generally aggregated at a token level to obtain a more intuitive overview of the influence of individual tokens.

Building upon this, Denil et al. (2015b) takes the input token vector and multiplies by the gradient (Input×Gradient), while Sundararajan et al. (2017b) compares the input with a null baseline input when computing the gradients w.r.t. the input (Integrated Gradients). Nielsen et al. (2022) offers a comprehensive overview of other propagation-based FAs.

Attention-based methods are applied to models that include an attention mechanism to weigh the input tokens. The assumption is that the attention weights represent the importance of each token. These FAs include scaling the attention weights by their gradients, taking the attention scores from the last layer, and recursively computing the attention in each layer (Serrano & Smith, 2019; Jain et al., 2020; Abnar & Zuidema, 2020).

Perturbation-based methods measure the difference in model prediction between using the original input and a corrupted version of the input by gradually removing tokens (Lei et al., 2016; Nguyen, 2018; Bastings et al., 2019; Bashier et al., 2020). The underlying idea is that removing important tokens will lead the model to flip its prediction or a significant drop in the prediction confidence. For instance, the input token at position i can be removed, and the resulting probability difference $\mathcal{F}_\theta(\mathrm{X}) - \mathcal{F}_\theta(\mathrm{X} \setminus x_i)$ can be used as an estimate for its importance. If the logit or probability given to the original output does not change, we conclude that the i-th token has no influence. Differently, some perturbation-based techniques utilize a modified model or a separate explainer model to learn feature attributions (Ribeiro et al., 2016; Lundberg & Lee, 2017; Bashier et al., 2020; Hase et al., 2021). LIME (Ribeiro et al., 2016) and SHAP (Lundberg & Lee, 2017) fall into this category.

7 Conclusion

In this paper, we introduced NOISER, a perturbation-based input attribution method that employs bounded noise to address the distribution shift problem arising from the discrete nature of text, aiming to explain language model predictions in generation tasks. Furthermore, we proposed *answerability* metrics, a novel automatic plausibility evaluation metric that leverages an LLM to evaluate the relevance of attributed rationales to the target output in the absence of gold rationales or human evaluation. Through comprehensive experiments across three tasks and six LLMs, we demonstrated that NOISER consistently surpasses existing baselines in terms of both faithfulness and answerability rate. Notably, our approach requires no supervision, positioning it as a promising direction for improving model interpretability and efficiency.

Acknowledgements

Reza was funded by the "*borsa di studio post laurea per attività di ricerca*" from the Department of Computer Science and Information Engineering of the University of Trento. Aryo Pradipta Gema was supported by the United Kingdom Research and Innovation (grant EP/S02431X/1), UKRI Centre for Doctoral Training in Biomedical AI at the University of Edinburgh, School of Informatics. Yu Zhao was supported by the UKRI Centre for Doctoral Training in Natural Language Processing, funded by UK Research and Innovation (grant EP/S022481/1). Pasquale Minervini was partially funded by ELIAI, an industry grant from Cisco, and a donation from Accenture LLP. This work was supported by the Edinburgh International Data Facility (EIDF) and the Data-Driven Innovation Programme at the University of Edinburgh. Gabriele is supported by the Dutch Research Council (NWO) as part of the InDeep project (NWA.1292.19.399). Andrea Passerini was partially funded by the TANGO project, funded by the Horizon Europe Programme, Grant Agreement no. 101120763. Funded by the European Union. Views and opinions expressed are however those of the author(s) only and do not necessarily reflect those of the European Union or the European Health and Digital Executive Agency (HaDEA). Neither the European Union nor the granting authority can be held responsible for them.

References

Samira Abnar and Willem Zuidema. Quantifying attention flow in transformers, 2020. URL https://arxiv.org/abs/2005.00928.

Leila Arras, Franziska Horn, Grégoire Montavon, Klaus-Robert Müller, and Wojciech Samek. "what is relevant in a text document?": An interpretable machine learning approach. *PLOS ONE*, 12(8):e0181142, August 2017. ISSN 1932-6203. doi: 10.1371/journal.pone.0181142. URL http://dx.doi.org/10.1371/journal.pone.0181142.

Pepa Atanasova, Jakob Grue Simonsen, Christina Lioma, and Isabelle Augenstein. A diagnostic study of explainability techniques for text classification. In *Proceedings of the 2020 Conference on Empirical Methods in Natural Language Processing (EMNLP)*, pp. 3256–3274, Online, November 2020. Association for Computational Linguistics. doi: 10.18653/v1/2020.emnlp-main.263. URL https://aclanthology.org/2020.emnlp-main.263.

Jinze Bai, Shuai Bai, Yunfei Chu, Zeyu Cui, Kai Dang, Xiaodong Deng, Yang Fan, Wenbin Ge, Yu Han, Fei Huang, Binyuan Hui, Luo Ji, Mei Li, Junyang Lin, Runji Lin, Dayiheng Liu, Gao Liu, Chengqiang Lu, Keming Lu, Jianxin Ma, Rui Men, Xingzhang Ren, Xuancheng Ren, Chuanqi Tan, Sinan Tan, Jianhong Tu, Peng Wang, Shijie Wang, Wei Wang, Shengguang Wu, Benfeng Xu, Jin Xu, An Yang, Hao Yang, Jian Yang, Shusheng Yang, Yang Yao, Bowen Yu, Hongyi Yuan, Zheng Yuan, Jianwei Zhang, Xingxuan Zhang, Yichang Zhang, Zhenru Zhang, Chang Zhou, Jingren Zhou, Xiaohuan Zhou, and Tianhang Zhu. Qwen technical report. *arXiv preprint arXiv:2309.16609*, 2023.

Housam Khalifa Bashier, Mi-Young Kim, and Randy Goebel. RANCC: Rationalizing neural networks via concept clustering. In *Proceedings of the 28th International Conference on Computational Linguistics*, pp. 3214–3224, Barcelona, Spain (Online), December 2020. International Committee on Computational Linguistics. doi: 10.18653/v1/2020.coling-main.286. URL https://aclanthology.org/2020.coling-main.286.

Jasmijn Bastings, Wilker Aziz, and Ivan Titov. Interpretable neural predictions with differentiable binary variables. In *Proceedings of the 57th Annual Meeting of the Association for Computational Linguistics*, pp. 2963–2977, Florence, Italy, July 2019. Association for Computational Linguistics. doi: 10.18653/v1/P19-1284. URL https://aclanthology.org/P19-1284.

Oana-Maria Camburu, Tim Rocktäschel, Thomas Lukasiewicz, and Phil Blunsom. e-snli: Natural language inference with natural language explanations. In S. Bengio, H. Wallach, H. Larochelle, K. Grauman, N. Cesa-Bianchi, and R. Garnett (eds.), *Advances in Neural Information Processing Systems*, volume 31. Curran Associates, Inc., 2018. URL https://proceedings.neurips.cc/paper_files/paper/2018/file/4c7a167bb329bd92580a99ce422d6fa6-Paper.pdf.

Aaron Chan, Maziar Sanjabi, Lambert Mathias, Liang Tan, Shaoliang Nie, Xiaochang Peng, Xiang Ren, and Hamed Firooz. UNIREX: A unified learning framework for language model rationale extraction. In *Proceedings of BigScience Episode #5 – Workshop on Challenges & Perspectives in Creating Large Language Models*, pp. 51–67, virtual+Dublin, May 2022a. Association for Computational Linguistics. doi: 10.18653/v1/2022.bigscience-1.5. URL https://aclanthology.org/2022.bigscience-1.5.

Chun Sik Chan, Huanqi Kong, and Liang Guanqing. A comparative study of faithfulness metrics for model interpretability methods. In *Proceedings of the 60th Annual Meeting of the Association for Computational Linguistics (Volume 1: Long Papers)*, pp. 5029–5038, Dublin, Ireland, May 2022b. Association for Computational Linguistics. doi: 10.18653/v1/2022.acl-long.345. URL https://aclanthology.org/2022.acl-long.345.

Lichang Chen, Shiyang Li, Jun Yan, Hai Wang, Kalpa Gunaratna, Vikas Yadav, Zheng Tang, Vijay Srinivasan, Tianyi Zhou, Heng Huang, and Hongxia Jin. Alpagasus: Training a better alpaca with fewer data, 2024. URL https://arxiv.org/abs/2307.08701.

George Chrysostomou and Nikolaos Aletras. Enjoy the salience: Towards better transformer-based faithful explanations with word salience. In *Proceedings of the 2021 Conference on Empirical Methods in Natural Language Processing*, pp. 8189–8200, Online and Punta Cana, Dominican Republic, November 2021. Association for Computational Linguistics. doi: 10.18653/v1/2021.emnlp-main.645. URL https://aclanthology.org/2021.emnlp-main.645.

George Chrysostomou and Nikolaos Aletras. An empirical study on explanations in out-of-domain settings. In *Proceedings of the 60th Annual Meeting of the Association for Computational Linguistics (Volume 1: Long Papers)*, pp. 6920–6938, Dublin, Ireland, May 2022. Association for Computational Linguistics. doi: 10.18653/v1/2022.acl-long.477. URL https://aclanthology.org/2022.acl-long.477.

DeepSeek-AI. Deepseek-r1: Incentivizing reasoning capability in llms via reinforcement learning, 2025. URL https://arxiv.org/abs/2501.12948.

Misha Denil, Alban Demiraj, and Nando de Freitas. Extraction of salient sentences from labelled documents, 2015a.

Misha Denil, Alban Demiraj, and Nando de Freitas. Extraction of salient sentences from labelled documents, 2015b. URL https://arxiv.org/abs/1412.6815.

Jay DeYoung, Sarthak Jain, Nazneen Fatema Rajani, Eric Lehman, Caiming Xiong, Richard Socher, and Byron C. Wallace. ERASER: A benchmark to evaluate rationalized NLP models. In *Proceedings of the 58th Annual Meeting of the Association for Computational Linguistics*, pp. 4443–4458, Online, July 2020. Association for Computational Linguistics. doi: 10.18653/v1/2020.acl-main.408. URL https://aclanthology.org/2020.acl-main.408.

Finale Doshi-Velez and Been Kim. Towards a rigorous science of interpretable machine learning, 2017.

Joseph Enguehard. Sequential integrated gradients: a simple but effective method for explaining language models, 2023. URL https://arxiv.org/abs/2305.15853.

Nils Feldhus, Leonhard Hennig, Maximilian Dustin Nasert, Christopher Ebert, Robert Schwarzenberg, and Sebastian Möller. Saliency map verbalization: Comparing feature importance representations from model-free and instruction-based methods. In Bhavana Dalvi Mishra, Greg Durrett, Peter Jansen, Danilo Neves Ribeiro, and Jason Wei (eds.), *Proceedings of the 1st Workshop on Natural Language Reasoning and Structured Explanations (NLRSE)*, pp. 30–46, Toronto, Canada, June 2023. Association for Computational Linguistics. doi: 10.18653/v1/2023.nlrse-1.4. URL https://aclanthology.org/2023.nlrse-1.4/.

Mohammad Reza Ghasemi Madani and Pasquale Minervini. REFER: An end-to-end rationale extraction framework for explanation regularization. In Jing Jiang, David Reitter, and Shumin Deng (eds.), *Proceedings of the 27th Conference on Computational Natural Language Learning (CoNLL)*, pp. 587–602, Singapore, December 2023. Association for Computational Linguistics. doi: 10.18653/v1/2023.conll-1.40. URL https://aclanthology.org/2023.conll-1.40.

Peter Hase, Harry Xie, and Mohit Bansal. The out-of-distribution problem in explainability and search methods for feature importance explanations, 2021. URL https://arxiv.org/abs/2106.00786.

Maksims Ivanovs, Roberts Kadikis, and Kaspars Ozols. Perturbation-based methods for explaining deep neural networks: A survey. *Pattern Recognition Letters*, 150:228–234, 2021. ISSN 0167-8655. doi: https://doi.org/10.1016/j.patrec.2021.06.030. URL https://www.sciencedirect.com/science/article/pii/S0167865521002440.

Alon Jacovi and Yoav Goldberg. Aligning faithful interpretations with their social attribution. *Transactions of the Association for Computational Linguistics*, 9:294–310, 2021. doi: 10.1162/tacl_a_00367. URL https://aclanthology.org/2021.tacl-1.18.

Sarthak Jain, Sarah Wiegreffe, Yuval Pinter, and Byron C. Wallace. Learning to faithfully rationalize by construction, 2020. URL https://arxiv.org/abs/2005.00115.

Tom Kersten, Hugh Mee Wong, Jaap Jumelet, and Dieuwke Hupkes. Attention vs non-attention for a shapley-based explanation method. In *Proceedings of Deep Learning Inside Out (DeeLIO): The 2nd Workshop on Knowledge Extraction and Integration for Deep Learning Architectures*, pp. 129–139, Online, June 2021. Association for Computational Linguistics. doi: 10.18653/v1/2021.deelio-1.13. URL https://aclanthology.org/2021.deelio-1.13.

Remi Lebret, David Grangier, and Michael Auli. Neural text generation from structured data with application to the biography domain, 2016. URL https://arxiv.org/abs/1603.07771.

Tao Lei, Regina Barzilay, and Tommi Jaakkola. Rationalizing neural predictions. In *Proceedings of the 2016 Conference on Empirical Methods in Natural Language Processing*, pp. 107–117, Austin, Texas, November 2016. Association for Computational Linguistics. doi: 10.18653/v1/D16-1011. URL https://aclanthology.org/D16-1011.

Xian Li, Ping Yu, Chunting Zhou, Timo Schick, Omer Levy, Luke Zettlemoyer, Jason Weston, and Mike Lewis. Self-alignment with instruction backtranslation, 2024. URL https://arxiv.org/abs/2308.06259.

Zachary C. Lipton. The mythos of model interpretability. *Commun. ACM*, 61(10):36–43, sep 2018. ISSN 0001-0782. doi: 10.1145/3233231. URL https://doi.org/10.1145/3233231.

Shusen Liu, Zhimin Li, Tao Li, Vivek Srikumar, Valerio Pascucci, and Peer-Timo Bremer. Nlize: A perturbation-driven visual interrogation tool for analyzing and interpreting natural language inference models. *IEEE Transactions on Visualization and Computer Graphics*, 25(1):651–660, January 2019. ISSN 1077-2626. doi: 10.1109/TVCG.2018.2865230. URL https://doi.org/10.1109/TVCG.2018.2865230.

Shayne Longpre, Le Hou, Tu Vu, Albert Webson, Hyung Won Chung, Yi Tay, Denny Zhou, Quoc V. Le, Barret Zoph, Jason Wei, and Adam Roberts. The flan collection: Designing data and methods for effective instruction tuning, 2023. URL https://arxiv.org/abs/2301.13688.

Scott Lundberg and Su-In Lee. A unified approach to interpreting model predictions, 2017. URL https://arxiv.org/abs/1705.07874.

Siwen Luo, Hamish Ivison, Caren Han, and Josiah Poon. Local interpretations for explainable natural language processing: A survey, 2022.

Andreas Madsen, Nicholas Meade, Vaibhav Adlakha, and Siva Reddy. Evaluating the faithfulness of importance measures in NLP by recursively masking allegedly important tokens and retraining. In Yoav Goldberg, Zornitsa Kozareva, and Yue Zhang (eds.), *Findings of the Association for Computational Linguistics: EMNLP 2022*, pp. 1731–1751, Abu Dhabi, United Arab Emirates, December 2022. Association for Computational Linguistics. doi: 10.18653/v1/2022.findings-emnlp.125. URL https://aclanthology.org/2022.findings-emnlp.125/.

Potsawee Manakul, Adian Liusie, and Mark J. F. Gales. Selfcheckgpt: Zero-resource black-box hallucination detection for generative large language models, 2023. URL https://arxiv.org/abs/2303.08896.

Kevin Meng, David Bau, Alex Andonian, and Yonatan Belinkov. Locating and editing factual associations in gpt, 2023. URL https://arxiv.org/abs/2202.05262.

Dong Nguyen. Comparing automatic and human evaluation of local explanations for text classification. In *Proceedings of the 2018 Conference of the North American Chapter of the Association for Computational Linguistics: Human Language Technologies, Volume 1 (Long Papers)*, pp. 1069–1078, New Orleans, Louisiana, June 2018. Association for Computational Linguistics. doi: 10.18653/v1/N18-1097. URL https://aclanthology.org/N18-1097.

Ian E. Nielsen, Dimah Dera, Ghulam Rasool, Ravi P. Ramachandran, and Nidhal Carla Bouaynaya. Robust explainability: A tutorial on gradient-based attribution methods for deep neural networks. *IEEE Signal Processing Magazine*, 39(4):73–84, July 2022. ISSN 1558-0792. doi: 10.1109/msp.2022.3142719. URL http://dx.doi.org/10.1109/MSP.2022.3142719.

OpenAI, Josh Achiam, Steven Adler, Sandhini Agarwal, Lama Ahmad, Ilge Akkaya, Florencia Leoni Aleman, Diogo Almeida, Janko Altenschmidt, Sam Altman, Shyamal Anadkat, Red Avila, Igor Babuschkin, Suchir Balaji, Valerie Balcom, Paul Baltescu, Haiming Bao, Mohammad Bavarian, Jeff Belgum, Irwan Bello, Jake Berdine, Gabriel Bernadett-Shapiro, Christopher Berner, Lenny Bogdonoff, Oleg Boiko, Madelaine Boyd, Anna-Luisa Brakman, Greg Brockman, Tim Brooks, Miles Brundage, Kevin Button, Trevor Cai, Rosie Campbell, Andrew Cann, Brittany Carey, Chelsea Carlson, Rory Carmichael, Brooke Chan, Che Chang, Fotis Chantzis, Derek Chen, Sully Chen, Ruby Chen, Jason Chen, Mark Chen, Ben Chess, Chester Cho, Casey Chu, Hyung Won Chung, Dave Cummings, Jeremiah Currier, Yunxing Dai, Cory Decareaux, Thomas Degry, Noah Deutsch, Damien Deville, Arka Dhar, David Dohan, Steve Dowling, Sheila Dunning, Adrien Ecoffet, Atty Eleti, Tyna Eloundou, David Farhi, Liam Fedus, Niko Felix, Simón Posada Fishman, Juston Forte, Isabella Fulford, Leo Gao, Elie Georges, Christian Gibson, Vik Goel, Tarun Gogineni, Gabriel Goh, Rapha Gontijo-Lopes, Jonathan Gordon, Morgan Grafstein, Scott Gray, Ryan Greene, Joshua Gross, Shixiang Shane Gu, Yufei Guo, Chris Hallacy, Jesse Han, Jeff Harris, Yuchen He, Mike Heaton, Johannes Heidecke, Chris Hesse, Alan Hickey, Wade Hickey, Peter Hoeschele, Brandon Houghton, Kenny Hsu, Shengli Hu, Xin Hu, Joost Huizinga, Shantanu Jain, Shawn Jain, Joanne Jang, Angela Jiang, Roger Jiang, Haozhun Jin, Denny Jin, Shino Jomoto, Billie Jonn, Heewoo Jun, Tomer Kaftan, Łukasz Kaiser, Ali Kamali, Ingmar Kanitscheider, Nitish Shirish Keskar, Tabarak Khan, Logan Kilpatrick, Jong Wook Kim, Christina Kim, Yongjik Kim, Jan Hendrik Kirchner, Jamie Kiros, Matt Knight, Daniel Kokotajlo, Łukasz Kondraciuk, Andrew Kondrich, Aris Konstantinidis, Kyle Kosic, Gretchen Krueger, Vishal Kuo, Michael Lampe, Ikai Lan, Teddy Lee, Jan Leike, Jade Leung, Daniel Levy, Chak Ming Li, Rachel Lim, Molly Lin, Stephanie Lin, Mateusz Litwin, Theresa Lopez, Ryan Lowe, Patricia Lue, Anna Makanju, Kim Malfacini, Sam Manning, Todor Markov, Yaniv Markovski, Bianca Martin, Katie Mayer, Andrew Mayne, Bob McGrew, Scott Mayer McKinney, Christine McLeavey, Paul McMillan, Jake McNeil, David Medina, Aalok Mehta, Jacob Menick, Luke Metz, Andrey Mishchenko, Pamela Mishkin, Vinnie Monaco, Evan Morikawa, Daniel Mossing, Tong Mu, Mira Murati, Oleg Murk, David Mély, Ashvin Nair, Reiichiro Nakano, Rajeev Nayak, Arvind Neelakantan, Richard Ngo, Hyeonwoo Noh, Long Ouyang, Cullen O'Keefe, Jakub Pachocki, Alex Paino, Joe Palermo, Ashley Pantuliano, Giambattista Parascandolo, Joel Parish, Emy Parparita, Alex Passos, Mikhail Pavlov, Andrew Peng, Adam Perelman, Filipe de Avila Belbute Peres, Michael Petrov, Henrique Ponde de Oliveira Pinto, Michael, Pokorny, Michelle Pokrass, Vitchyr H. Pong, Tolly Powell, Alethea Power, Boris Power, Elizabeth Proehl, Raul Puri, Alec Radford, Jack Rae, Aditya Ramesh, Cameron Raymond, Francis Real, Kendra Rimbach, Carl Ross, Bob Rotsted, Henri Roussez, Nick Ryder, Mario Saltarelli, Ted Sanders, Shibani Santurkar, Girish Sastry, Heather Schmidt, David Schnurr, John Schulman, Daniel Selsam, Kyla Sheppard, Toki Sherbakov, Jessica Shieh, Sarah Shoker, Pranav Shyam, Szymon Sidor, Eric Sigler, Maddie Simens, Jordan Sitkin, Katarina Slama, Ian Sohl, Benjamin Sokolowsky, Yang Song, Natalie Staudacher, Felipe Petroski Such, Natalie Summers, Ilya Sutskever, Jie Tang, Nikolas Tezak, Madeleine B. Thompson, Phil Tillet, Amin Tootoonchian, Elizabeth Tseng, Preston Tuggle, Nick Turley, Jerry Tworek, Juan Felipe Cerón Uribe, Andrea Vallone, Arun Vijayvergiya, Chelsea Voss, Carroll Wainwright, Justin Jay Wang, Alvin Wang, Ben Wang, Jonathan Ward, Jason Wei, CJ Weinmann, Akila Welihinda, Peter Welinder, Jiayi Weng, Lilian Weng, Matt Wiethoff, Dave Willner, Clemens Winter, Samuel Wolrich, Hannah Wong, Lauren Workman, Sherwin Wu, Jeff Wu, Michael Wu, Kai Xiao, Tao Xu, Sarah Yoo, Kevin Yu, Qiming Yuan, Wojciech Zaremba, Rowan Zellers, Chong Zhang, Marvin Zhang, Shengjia Zhao, Tianhao Zheng, Juntang Zhuang, William Zhuk, and Barret Zoph. Gpt-4 technical report, 2024. URL https://arxiv.org/abs/2303.08774.

Baolin Peng, Chunyuan Li, Pengcheng He, Michel Galley, and Jianfeng Gao. Instruction tuning with gpt-4, 2023. URL https://arxiv.org/abs/2304.03277.

Yiwei Qin, Kaiqiang Song, Yebowen Hu, Wenlin Yao, Sangwoo Cho, Xiaoyang Wang, Xuansheng Wu, Fei Liu, Pengfei Liu, and Dong Yu. Infobench: Evaluating instruction following ability in large language models, 2024. URL https://arxiv.org/abs/2401.03601.

Nazneen Fatema Rajani, Bryan McCann, Caiming Xiong, and Richard Socher. Explain yourself! leveraging language models for commonsense reasoning. In *Proceedings of the 57th Annual Meeting of the Association for Computational Linguistics*, pp. 4932–4942, Florence, Italy, July 2019. Association for Computational Linguistics. doi: 10.18653/v1/P19-1487. URL https://aclanthology.org/P19-1487.

Marco Tulio Ribeiro, Sameer Singh, and Carlos Guestrin. "why should i trust you?": Explaining the predictions of any classifier, 2016. URL https://arxiv.org/abs/1602.04938.

Cynthia Rudin. Stop explaining black box machine learning models for high stakes decisions and use interpretable models instead, 2019.

Gabriele Sarti, Nils Feldhus, Ludwig Sickert, Oskar van der Wal, Malvina Nissim, and Arianna Bisazza. Inseq: An interpretability toolkit for sequence generation models. In *Proceedings of the 61st Annual Meeting of the Association for Computational Linguistics*

(Volume 3: System Demonstrations), pp. 421–435, Toronto, Canada, July 2023. Association for Computational Linguistics. doi: 10.18653/v1/2023.acl-demo.40. URL https://aclanthology.org/2023.acl-demo.40.

Gabriele Sarti, Nils Feldhus, Jirui Qi, Malvina Nissim, and Arianna Bisazza. Democratizing advanced attribution analyses of generative language models with the inseq toolkit. In *xAI-2024 Late-breaking Work, Demos and Doctoral Consortium Joint Proceedings*, pp. 289–296, Valletta, Malta, July 2024. CEUR.org. URL https://ceur-ws.org/Vol-3793/paper_37.pdf.

Sofia Serrano and Noah A. Smith. Is attention interpretable? In *Proceedings of the 57th Annual Meeting of the Association for Computational Linguistics*, pp. 2931–2951, Florence, Italy, July 2019. Association for Computational Linguistics. doi: 10.18653/v1/P19-1282. URL https://aclanthology.org/P19-1282.

Avanti Shrikumar, Peyton Greenside, and Anshul Kundaje. Learning important features through propagating activation differences, 2019. URL https://arxiv.org/abs/1704.02685.

Mukund Sundararajan, Ankur Taly, and Qiqi Yan. Axiomatic attribution for deep networks, 2017a.

Mukund Sundararajan, Ankur Taly, and Qiqi Yan. Axiomatic attribution for deep networks, 2017b. URL https://arxiv.org/abs/1703.01365.

Rohan Taori, Ishaan Gulrajani, Tianyi Zhang, Yann Dubois, Xuechen Li, Carlos Guestrin, Percy Liang, and Tatsunori B. Hashimoto. Stanford alpaca: An instruction-following llama model. https://github.com/tatsu-lab/stanford_alpaca, 2023.

Gemma Team, Thomas Mesnard, Cassidy Hardin, Robert Dadashi, Surya Bhupatiraju, Shreya Pathak, Laurent Sifre, Morgane Rivière, Mihir Sanjay Kale, Juliette Love, Pouya Tafti, Léonard Hussenot, Pier Giuseppe Sessa, Aakanksha Chowdhery, Adam Roberts, Aditya Barua, Alex Botev, Alex Castro-Ros, Ambrose Slone, Amélie Héliou, Andrea Tacchetti, Anna Bulanova, Antonia Paterson, Beth Tsai, Bobak Shahriari, Charline Le Lan, Christopher A. Choquette-Choo, Clément Crepy, Daniel Cer, Daphne Ippolito, David Reid, Elena Buchatskaya, Eric Ni, Eric Noland, Geng Yan, George Tucker, George-Christian Muraru, Grigory Rozhdestvenskiy, Henryk Michalewski, Ian Tenney, Ivan Grishchenko, Jacob Austin, James Keeling, Jane Labanowski, Jean-Baptiste Lespiau, Jeff Stanway, Jenny Brennan, Jeremy Chen, Johan Ferret, Justin Chiu, Justin Mao-Jones, Katherine Lee, Kathy Yu, Katie Millican, Lars Lowe Sjoesund, Lisa Lee, Lucas Dixon, Machel Reid, Maciej Mikuła, Mateo Wirth, Michael Sharman, Nikolai Chinaev, Nithum Thain, Olivier Bachem, Oscar Chang, Oscar Wahltinez, Paige Bailey, Paul Michel, Petko Yotov, Rahma Chaabouni, Ramona Comanescu, Reena Jana, Rohan Anil, Ross McIlroy, Ruibo Liu, Ryan Mullins, Samuel L Smith, Sebastian Borgeaud, Sertan Girgin, Sholto Douglas, Shree Pandya, Siamak Shakeri, Soham De, Ted Klimenko, Tom Hennigan, Vlad Feinberg, Wojciech Stokowiec, Yu hui Chen, Zafarali Ahmed, Zhitao Gong, Tris Warkentin, Ludovic Peran, Minh Giang, Clément Farabet, Oriol Vinyals, Jeff Dean, Koray Kavukcuoglu, Demis Hassabis, Zoubin Ghahramani, Douglas Eck, Joelle Barral, Fernando Pereira, Eli Collins, Armand Joulin, Noah Fiedel, Evan Senter, Alek Andreev, and Kathleen Kenealy. Gemma: Open models based on gemini research and technology, 2024. URL https://arxiv.org/abs/2403.08295.

Hugo Touvron, Thibaut Lavril, Gautier Izacard, Xavier Martinet, Marie-Anne Lachaux, Timothée Lacroix, Baptiste Rozière, Naman Goyal, Eric Hambro, Faisal Azhar, Aurelien Rodriguez, Armand Joulin, Edouard Grave, and Guillaume Lample. Llama: Open and efficient foundation language models, 2023. URL https://arxiv.org/abs/2302.13971.

Keyon Vafa, Yuntian Deng, David M. Blei, and Alexander M. Rush. Rationales for sequential predictions, 2021. URL https://arxiv.org/abs/2109.06387.

Ashish Vaswani, Noam Shazeer, Niki Parmar, Jakob Uszkoreit, Llion Jones, Aidan N. Gomez, Lukasz Kaiser, and Illia Polosukhin. Attention is all you need, 2023. URL https://arxiv.org/abs/1706.03762.

Eric Wallace, Matt Gardner, and Sameer Singh. Interpreting predictions of NLP models. In *Proceedings of the 2020 Conference on Empirical Methods in Natural Language Processing: Tutorial Abstracts*, pp. 20–23, Online, November 2020. Association for Computational Linguistics. doi: 10.18653/v1/2020.emnlp-tutorials.3. URL https://aclanthology.org/2020.emnlp-tutorials.3.

Can Xu, Qingfeng Sun, Kai Zheng, Xiubo Geng, Pu Zhao, Jiazhan Feng, Chongyang Tao, and Daxin Jiang. Wizardlm: Empowering large language models to follow complex instructions, 2023. URL https://arxiv.org/abs/2304.12244.

Omar Zaidan, Jason Eisner, and Christine Piatko. Using "annotator rationales" to improve machine learning for text categorization. In *Human Language Technologies 2007: The Conference of the North American Chapter of the Association for Computational Linguistics; Proceedings of the Main Conference*, pp. 260–267, Rochester, New York, April 2007. Association for Computational Linguistics. URL https://aclanthology.org/N07-1033.

Matthew D. Zeiler and Rob Fergus. Visualizing and understanding convolutional networks. In David Fleet, Tomas Pajdla, Bernt Schiele, and Tinne Tuytelaars (eds.), *Computer Vision – ECCV 2014*, pp. 818–833, Cham, 2014. Springer International Publishing.

Hao Zhao, Maksym Andriushchenko, Francesco Croce, and Nicolas Flammarion. Long is more for alignment: A simple but tough-to-beat baseline for instruction fine-tuning, 2024. URL https://arxiv.org/abs/2402.04833.

Zhixue Zhao and Nikolaos Aletras. Incorporating attribution importance for improving faithfulness metrics. In Anna Rogers, Jordan Boyd-Graber, and Naoaki Okazaki (eds.), *Proceedings of the 61st Annual Meeting of the Association for Computational Linguistics (Volume 1: Long Papers)*, pp. 4732–4745, Toronto, Canada, July 2023. Association for Computational Linguistics. doi: 10.18653/v1/2023.acl-long.261. URL https://aclanthology.org/2023.acl-long.261.

Zhixue Zhao and Boxuan Shan. Reagent: A model-agnostic feature attribution method for generative language models, 2024. URL https://arxiv.org/abs/2402.00794.

Lianmin Zheng, Wei-Lin Chiang, Ying Sheng, Siyuan Zhuang, Zhanghao Wu, Yonghao Zhuang, Zi Lin, Zhuohan Li, Dacheng Li, Eric P. Xing, Hao Zhang, Joseph E. Gonzalez, and Ion Stoica. Judging llm-as-a-judge with mt-bench and chatbot arena, 2023. URL https://arxiv.org/abs/2306.05685.

Chunting Zhou, Pengfei Liu, Puxin Xu, Srini Iyer, Jiao Sun, Yuning Mao, Xuezhe Ma, Avia Efrat, Ping Yu, Lili Yu, Susan Zhang, Gargi Ghosh, Mike Lewis, Luke Zettlemoyer, and Omer Levy. Lima: Less is more for alignment, 2023a. URL https://arxiv.org/abs/2305.11206.

Jeffrey Zhou, Tianjian Lu, Swaroop Mishra, Siddhartha Brahma, Sujoy Basu, Yi Luan, Denny Zhou, and Le Hou. Instruction-following evaluation for large language models, 2023b. URL https://arxiv.org/abs/2311.07911.

A Soft-NC and Soft-NS Metrics

The Soft-NC and Soft-NS metrics are defined as follows:

$$\text{Soft-C}(\mathrm{X}, \hat{y}, \mathrm{X}') = \max(0, p(\hat{y} \mid \mathrm{X}) - p(\hat{y} \mid \mathrm{X}')) \tag{1}$$

$$\text{Soft-S}(\mathrm{X}, \hat{y}, \mathrm{X}') = 1 - \text{Soft-C}(\mathrm{X}, \hat{y}, \mathrm{X}') \tag{2}$$

where X' is soft-perturbed versions of X given the following instruction. For the embedding vector $\mathrm{x}_i \in \mathrm{X}$ and its FA score s_i, we modify the elements of x_i using Equation (3).

$$\mathrm{x}'_i = \mathrm{x}_i \odot \mathrm{e}_i, \quad \mathrm{e}_i \sim \text{Bernoulli}(q) \tag{3}$$

where e is a binary mask vector of size n (embedding size) and Bernoulli is parameterized with probability q:

$$q = \begin{cases} s, & \text{if retaining elements} \\ 1 - s, & \text{if removing elements} \end{cases} \tag{4}$$

The normalized sufficiency and comprehensiveness are then computed using the following equations:

$$\text{Soft-NC}(\mathrm{X}, \hat{y}, \mathrm{X}') = \frac{\text{Soft-C}(\mathrm{X}, \hat{y}, \mathrm{X}')}{1 - S(\mathrm{X}, \hat{y}, 0)} \tag{5}$$

$$\text{Soft-NS}(\mathrm{X}, \hat{y}, \mathrm{X}') = \frac{\text{Soft-S}(\mathrm{X}, \hat{y}, \mathrm{X}') - S(\mathrm{X}, \hat{y}, 0)}{1 - S(\mathrm{X}, \hat{y}, 0)} \tag{6}$$

However, in generation tasks, the absence of a predictive likelihood for the predicted label makes applying Soft-NS and Soft-NC challenging. Zhao & Aletras (2023) proposed using the Hellinger distance between prediction distributions over the vocabulary as a measure of changes in model predictions. They substitute $p(\hat{y} \mid \mathrm{X}) - p(\hat{y} \mid \mathrm{X}')$ in Equation (1) with the Hellinger distance. Given two discrete probability distributions, $P_{\mathrm{X},t} = [p_{1,t}, \ldots, p_{v,t}]$ and $P_{\mathrm{X}',t} = [p'_{1,t}, \ldots, p'_{v,t}]$, the Hellinger distance is formally defined as:

$$\Delta P_{\mathrm{X}',t} = H(P_{\mathrm{X},t}, P_{\mathrm{X}',t}) = \frac{1}{\sqrt{2}} \cdot \sqrt{\sum_{i=1}^{v} \left(\sqrt{p_{i,t}} - \sqrt{p'_{i,t}}\right)^2}$$

where $P_{\mathrm{X},t}$ is the probability distribution over the entire vocabulary (of size v) when prompting the model with the full-text X. $P_{\mathrm{X}',t}$ is for prompting the model with soft-perturbed text. For a given sequence input X and a model of vocabulary size v, at time step t, the model generates a distribution $P_{\mathrm{X},t}$ for the next token x_T. The final Soft-NS and Soft-NC at step t for text generation are formulated as:

$$\text{Soft-NS}(\mathrm{X}, x_t, \mathcal{R}) = \frac{\max(0, \Delta P_{0,t} - \Delta P_{\mathrm{X}',t})}{\Delta P_{0,t}} \tag{7}$$

$$\text{Soft-NC}(\mathrm{X}, x_t, \mathcal{R}) = \frac{\Delta P_{\mathrm{X}' \setminus \mathcal{R},t}}{\Delta P_{0,t}} \tag{8}$$

where $\Delta P_{0,t}$ is Hellinger's distance between a zero input's probability distribution and full-text input's probability distribution. $\mathrm{X}' \setminus \mathcal{R}$ is the case of "if removing elements" described in Equation (4).

B More Results

Table 5 provides the detailed Soft-NS and Soft-NC scores of our experiments.

Table 6 illustrates the answerability metrics on top-50% of feature attributions given the judge model top-5 predictions.

We also analyzed the correlation between the faithfulness score and the answerability metrics on KNOWN in Figure 4. The results show that IG, SHAP, DeepLIFT, IxG, LIME, and Occlusion exhibit similar faithfulness scores, with Occlusion achieving the highest answerability rate and score among them. Meanwhile, NOISER surpasses all baselines in both faithfulness and answerability score but falls short in answerability rate, trailing Occlusion by 5%.

KNOWN

Method	Qwen2-0.5B		Llama3.2-1b		Qwen2-1.5B		gemma-2-2b		gemma-2-9b		Llama3-8b	
	Soft-NS	Soft-NC	Soft-NS	Soft-NC	Soft-NS	Soft-NC	Soft-NS	Soft-NC	Soft-NS	Soft-NC	Soft-NS	Soft-NC
Last Attn	0.0372	-0.1229	-0.0301	-0.0301	0.0023	0.0584	0.1617	-0.0211	0.0321	-0.3109	-0.1148	0.1052
Rollout	-0.2567	0.1406	-0.0426	-0.0045	-0.0264	0.1475	0.3582	0.1042	0.0114	-0.3721	-0.5818	0.3194
SHAP	-0.2714	0.7660	-0.1643	0.5388	-0.0809	0.6199	-0.0050	0.3776	0.1933	0.7270	-0.3386	0.5310
IxG	-0.5373	0.7490	0.0079	0.6980	-0.0843	0.5455	-0.1152	0.6384	-0.0265	1.0541	0.0750	0.5141
IG	-0.6136	0.8312	-0.1202	0.6629	-0.1209	0.6372	-0.1328	0.3343	0.1540	0.8815	-0.3386	0.7144
DeepLIFT	-0.5430	0.8460	-0.0801	0.6274	-0.0826	0.6149	-0.1296	0.4853	-0.0109	0.8747	0.0147	0.5027
SIG	-0.4989	0.5350	-0.0841	0.4375	-0.0964	0.3969	-0.1494	-0.0385	0.1730	0.6147	-0.1886	0.4640
LIME	-0.0221	0.2660	0.2210	0.2920	0.0678	0.3149	0.1336	0.2230	0.2100	0.2732	0.5459	0.1096
Occlusion	0.1138	0.0489	0.2267	0.3105	0.0606	0.1872	0.1830	0.3510	0.2119	0.3102	0.8302	-0.0470
NOISER	0.6785	1.5068	0.2248	1.1741	-0.0264	1.4664	0.1805	1.2627	-0.0233	2.2001	0.8043	1.4133

LONGRA

Method	Qwen2-0.5B		Llama3.2-1b		Qwen2-1.5B		gemma-2-2b		gemma-2-9b		Llama3-8b	
	Soft-NS	Soft-NC	Soft-NS	Soft-NC	Soft-NS	Soft-NC	Soft-NS	Soft-NC	Soft-NS	Soft-NC	Soft-NS	Soft-NC
Last Attn	1.8502	0.0645	0.2522	0.0733	0.0828	-0.0938	-0.1583	-0.0799	-0.1583	-0.0799	0.0888	0.9874
Rollout	1.8541	-0.0025	0.0894	0.1557	0.0927	-0.0126	-0.1790	-0.0853	-0.1790	-0.0853	0.1052	1.1231
SHAP	1.5203	2.2767	-0.3437	1.6274	-0.0323	1.6599	0.1364	1.8382	0.1444	2.1325	-0.4277	1.1972
IxG	1.3174	2.5798	-0.1419	1.8718	-0.0682	1.6052	0.2919	2.2883	0.2919	2.2883	0.1390	1.9406
IG	1.5378	2.8010	-0.3141	1.6207	-0.1039	1.6537	0.3475	0.9548	0.3475	0.9548	0.0639	3.6551
DeepLIFT	1.6777	2.8214	-0.0546	1.8435	-0.1606	1.7118	0.2430	2.4998	0.2430	2.4998	0.0657	2.0600
SIG	2.4897	1.3749	-0.3132	1.2404	-0.0297	1.1344	0.1009	0.4404	0.1009	0.4404	0.1895	0.9723
LIME	0.9895	0.0870	0.1343	0.0869	-0.4042	-0.0106	-0.0112	-0.1524	-0.0112	-0.1524	0.0923	2.2071
Occlusion	2.2561	1.6862	0.1370	1.8517	-0.4008	1.4153	0.5531	2.8887	0.5531	2.8887	-0.0124	4.2364
NOISER	2.0935	4.7119	0.3242	4.4831	-0.9588	4.1367	0.5164	3.7563	1.1446	5.0235	0.4705	4.6922

WIKIBIO

Method	Qwen2-0.5B		Llama3.2-1b		Qwen2-1.5B		gemma-2-2b		gemma-2-9b		Llama3-8b	
	Soft-NS	Soft-NC	Soft-NS	Soft-NC	Soft-NS	Soft-NC	Soft-NS	Soft-NC	Soft-NS	Soft-NC	Soft-NS	Soft-NC
Last Attn	0.8145	0.2459	0.1041	0.5263	0.0126	-0.7181	-0.1474	-0.1105	0.2246	0.0569	-0.0905	0.6405
Rollout	-0.6789	0.0385	0.0254	0.5336	0.0424	-0.7490	-0.0168	0.5253	0.2655	0.0843	-0.2114	1.0899
SHAP	0.6624	0.8078	0.0470	1.1202	-0.0263	1.1476	0.0071	0.7895	0.4254	2.7240	-0.0304	1.4368
IxG	1.1577	2.2695	0.0991	1.7374	0.2109	1.1833	0.0320	1.5496	0.4097	2.1950	0.2509	1.1238
IG	0.5209	1.9008	0.0047	1.5749	-0.0232	0.7207	-0.0408	1.2318	0.5993	3.5124	-0.4283	1.1159
DeepLIFT	0.9232	2.2975	-0.0490	1.6755	0.0495	1.4096	0.0574	1.4033	0.3253	1.9753	0.1346	1.1393
SIG	1.4616	2.3040	-0.1815	1.6114	0.3493	1.7323	0.1572	1.2684	0.9031	4.3250	0.6571	0.7049
LIME	1.6490	1.3519	0.1118	0.4537	0.1616	1.0099	0.1260	0.5920	0.7893	2.1634	0.3183	0.5166
Occlusion	2.6100	2.4950	0.3736	1.6283	0.9353	2.9564	0.4595	2.2637	1.3045	3.6255	1.5924	1.7961
NOISER	4.3005	4.4619	0.6959	3.0427	0.9847	4.0016	0.7941	3.4586	1.5671	5.5837	1.4975	3.1114

Table 5: Soft-NS and Soft-NC Scores Across Datasets.

Method	Qwen2-0.5B		Llama3.2-1b		Qwen2-1.5B		gemma-2-2b		gemma-2-9b		Llama3-8b		Average	
	Rate	Score	Rate	Score	Rate	Score	Rate	Score	Rate	Score	Rate	Score	Rate	Score
Last Attn	26%	0.1722	58%	0.3037	21%	0.1432	55%	0.2917	51%	0.2529	48%	0.2568	43%	0.2368
Rollout	21%	0.1445	37%	0.1836	23%	0.1604	23%	0.1086	36%	0.1621	40%	0.1980	30%	0.1595
SHAP	47%	0.3904	52%	0.3440	47%	0.3662	31%	0.2188	28%	0.2051	43%	0.2427	41%	0.2945
IxG	51%	0.4087	58%	0.4299	40%	0.3057	55%	0.3792	47%	0.3369	44%	0.3062	49%	0.3611
IG	48%	0.4004	54%	0.3586	43%	0.3367	31%	0.2308	25%	0.1847	42%	0.2172	41%	0.2881
DeepLIFT	49%	0.4138	60%	0.4067	40%	0.3159	48%	0.3271	45%	0.3164	44%	0.2898	48%	0.3450
SIG	40%	0.3025	44%	0.2759	40%	0.3091	24%	0.1644	36%	0.2698	28%	0.1584	35%	0.2467
LIME	49%	0.3936	49%	0.3315	53%	0.4307	61%	0.4021	60%	0.3916	48%	0.3230	53%	0.3787
Occlusion	**67%**	0.4666	**61%**	0.4001	**65%**	0.5093	64%	0.4204	**63%**	0.4043	**57%**	0.4241	**63%**	0.4375
NOISER	65%	**0.5996**	58%	**0.5435**	57%	**0.5474**	**66%**	**0.6245**	60%	**0.5400**	54%	**0.5962**	60%	**0.5752**

Table 6: Answerability metrics on KNOWN dataset w.r.t judge model **top-5** predictions.

C Datasets Statistics

Appendix C shows the number of true predictions by each model given KNOWN and LONGRA datasets.

Dataset	Qwen2-0.5B	Llama3.2-1b	Qwen2-1.5B	gemma-2-2b	gemma-2-9b	Llama3-8b
Known (1208)	661	828	774	830	822	875
LongRA (573)	140	160	170	209	148	165

Table 7: Number of true predictions captured by each model.

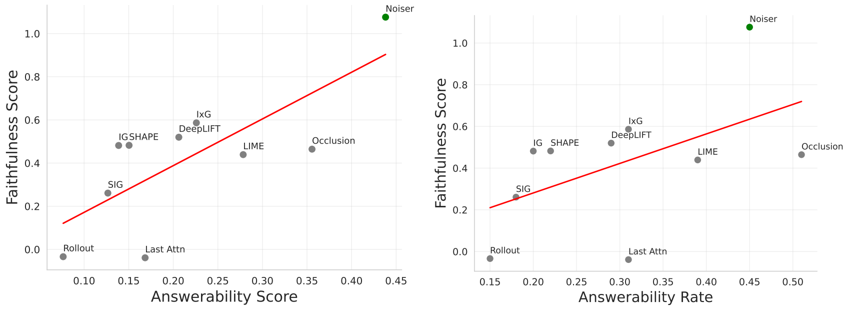

(a)

(b)

Figure 4: Comparison of average faithfulness score with (a) average answerability score and (b) answerability rate.

D Bounding Computations

Since $k_{\min}$ is dependent on the model, we introduce norm-bounding as the norm value of the noise vector $\mathbf{n}$ is different based on the model's embedding size (d_{model}). To avoid different norm values for each sample in a given data, we use the expected norm value of the noise vector, $\mathbb{E}\left[\|\mathbf{n}\|_p\right]$, and use $k = \frac{1}{\mathbb{E}\left[\|\mathbf{n}\|_p\right]}$ as the final bounding for the noise vector. In the following, we show the expected value of each norm given a model with d_{model} embedding dimensions.

Let $\mathbf{n} \in \mathbb{R}^{d_{\text{model}}}$ be a random vector where each component $n_i \sim \mathcal{N}(0,1)$. Below, we derive the expected values of different norms and compare their properties.

The L_2 norm (Euclidean Norm) is defined as follows:

$$\|\mathbf{n}\|_2 = \sqrt{\sum_{i=1}^{d_{\text{model}}} n_i^2}$$

where each n_i^2 follows a *chi-squared distribution* with 1 degree of freedom, which results in the following:

$$\mathbb{E}\left[\|\mathbf{n}\|_2^2\right] = d_{\text{model}}$$

By Jensen's inequality and the Law of Large Numbers, for large d_{model}:

$$\mathbb{E}\left[\|\mathbf{n}\|_2\right] \approx \sqrt{\mathbb{E}\left[\|\mathbf{n}\|_2^2\right]} = \sqrt{d_{\text{model}}}$$

The L_∞ norm (Maximum Norm) is defined as follows:

$$\|\mathbf{n}\|_\infty = \max_{1 \le i \le d_{\text{model}}} |n_i|$$

The cumulative distribution function (CDF) for $|n_i|$ is $F(x) = \operatorname{erf}\left(\frac{x}{\sqrt{2}}\right)$. The CDF for the maximum of d_{model} samples is $F_{\max}(x) = [F(x)]^{d_{\text{model}}}$. Using extreme value theory, the expected maximum for large d_{model} approximates:

$$\mathbb{E}\left[\|\mathbf{n}\|_\infty\right] \approx \sqrt{2 \ln d_{\text{model}}}$$

E Answerability Evaluation Prompt

Below, we provide the prompt used for evaluating FAs' answerability.

Answerability Evaluation Prompt

# Task:
Given a set of words extracted from a prompt for a completion task, return a single word as the most probable completion for the unseen prompt WITHOUT providing any explanation.